Coherent Fringe Tracking and Visibility Estimation for MIDI

Walter Jaffe

http://www.strw.leidenuniv.nl/Leiden Observatory, P.O. Box 9513, 2300 RA, Leiden, Netherlands;

ABSTRACT

We describe and illustrate the techniques used on spectrally dispersed data from the MIDI interferometer to estimate and remove variations in the atmospheric delay and dispersion. The resulting interferograms can then be added coherently yielding estimates of spectral correlated flux and differential phase. The primary advantage over incoherent estimation of correlated flux is that the system noise need not be accurately known.

Keywords: Infrared Interferometry, reduction techniques, Visibility Estimation

1. INTRODUCTION

The currently most common technique for estimating visibilities with optical/IR (OIR) interferometers is to scan the broad-band fringe by modulating the optical path difference (OPD), then filtering the fringe according to *a priori* estimates of the intended and unintended (atmospheric) contributions to the OPD rate, and finally measuring the total power (average amplitude squared) in the resulting fringe. The total power of all measured scans is then averaged, and an estimate of extraneous noise sources is subtracted. Dividing this estimate of the squared fringe power by separate measurements of the squared non-interferometric (photometric) flux yields an estimate of the squared visibility.

This procedure allows the summing of scans where the relative OPD is not known, and more importantly where the relative OPD velocity (due to atmospheric terms) is not precisely known.

In the N-band of the thermal IR (7-14μ), an attractive alternative is to disperse the photons and measure the fringe in frequency space rather than in OPD space. The advantages of the N-band for this purpose are that it is relatively broad ($\Delta\nu/\nu \sim 0.7$) and that the noise is primarily background photon Poisson noise. The broad band means that OPDs can be estimated from the spectrum with relatively high accuracy and small aliasing. The high background means that spectra can be measured rapidly and with moderate dispersion without the loss of signal/noise that occurs in the readout-noise limited regime. In this mode the OPD can be measured from a single exposure, the restriction on the atmospheric stability is roughly that the coherence time be longer than a single frame, rather than the fringe packet scan time.

Once all frames are reduced to the same OPD, they can be added coherently. Providing that the OPD reduction was accurate, this has the major advantages that the noise in the sum is (nearly) zero mean, the complex visibility can be estimated directly (modulo a linear phase gradient), and thus it is usually not necessary to subtract an estimate of the system noise from the visibility estimate.

The rest of this paper shows the detailed steps of coherent reduction of MIDI data, and discusses some of the limitations of the method.

Further author information: (Send correspondence to W.J.)
W.J.: E-mail: jaffe@strw.leidenuniv.nl, Telephone: +31 71 5275862

2. FRINGE DETECTION IN FREQUENCY SPACE

The output of a 2-port interferometer like MIDI is:

$$S(D) \quad = \quad \text{GARBAGE} \quad + \quad \int V(k)B(k)\cos(kD + \phi_v + \phi_i + \phi_a)\; dk$$

where D is the OPD, k is the spatial frequency $2\pi/\lambda$, $V(k)$ is the correlated flux, $B(k)$ is the frequency response of the interferometer,ϕ_v, ϕ_i and ϕ_a are source, instrumental, and atmospheric phase terms, and GARBAGE is an enormous amount of more or less slowly varying background, often > 100 times the signal, imposed by the sky, telescope, and instrument. To actually observe the fringe against this background it is necessary to modulate the signal. This can be done by modulating D with movable mirrors, or by dispersing the signal and looking at $S(D,k) = V(k)B(k)\cos(kD)$.

More generally D is the sum of D_i and D_a, the known instrumental delay and the unknown atmospheric delay, both variable. To find VB we could either measure a large number of almost random values of D and estimate $(VB)^2 \sim 2\times < S^2 >$, since $< \cos^2 > \sim 1/2$. This is basic incoherent estimation. Alternatively, we can try to guess D and demodulate the cosine. We construct the *delay function* $F(D')$ by a Fourier Transform:

$$F(D') \quad = \quad \int S(k)\exp(i\; kD')\; dk$$

Since

$$\cos(kD) \quad \equiv \quad (\exp(i\; kD)\; + \exp(-i\; kD))/2$$

in the case of an infinitely broad band and constant VB,

$$F(D') \quad = \quad (\delta(D' - D)\; + \; \delta(D' + D))/2$$

with two sharp peaks. With finite B or variable V these peaks will be broader. We can suppress the ambiguous sideband peak by modulating the instrumental delay D_i and demodulating the result: if $D = D_i + D_a$ and $S' = S\exp(-i\; kD_i)$ then:

$$F'(D') \quad = \quad (\delta(D' - D_a)\; + \; \delta(D' + D_a + 2D_i))/2$$

If we change D_i more rapidly than D_a changes, and average a few of the results, the first terms add constructively and the second terms do not, so the two peaks are distinguishable. Once we know D_a we can directly estimate $V(k)B(k)$

3. STEPS TO THE VISIBILITY ESTIMATE

MIDI[1] records N-band data from the VLTInteferometer[2] with a dispersion ($\lambda/\delta\lambda$) of ~ 25 (PRISM mode) or ~ 240 (GRISM mode). The data is read off a 320x240 Raytheon detector at about 50 Hz in the form of multiple *windows*, each recording a 2-dimensional spectrum from one of the beam combiner channels. Between each frame a set of piezo-driven mirrors modulates the *instrumental* OPD (D_i) in a repeated programmed cycle of steps, e.g. 20 steps of 2 microns. Typically an observation includes a few thousand frames.

3.1. Data Compression

The first step of the reduction is **data compression**; each of the two interferometric spectra are collapsed by multiplying by a weighting mask and summing in the spatial direction. Since the two ports of the beam combiner are essentially 180 degrees out of phase, they are subtracted to yield a single 1-d spectrum. About 90% of the **GARBAGE** is common mode between the two channels, and disappears in this step. An example of the output of this step is shown in Figure 1a. Here 1000 spectra, about 200 sec of data, are shown, with spectral channel on the vertical axis, and frame number/time on the horizontal axis. You can see almost nothing interesting in this Figure, because the signal is still dominated by thermal and instrumental backgrounds. In Fig 1b we plot a single spectrum from this series.

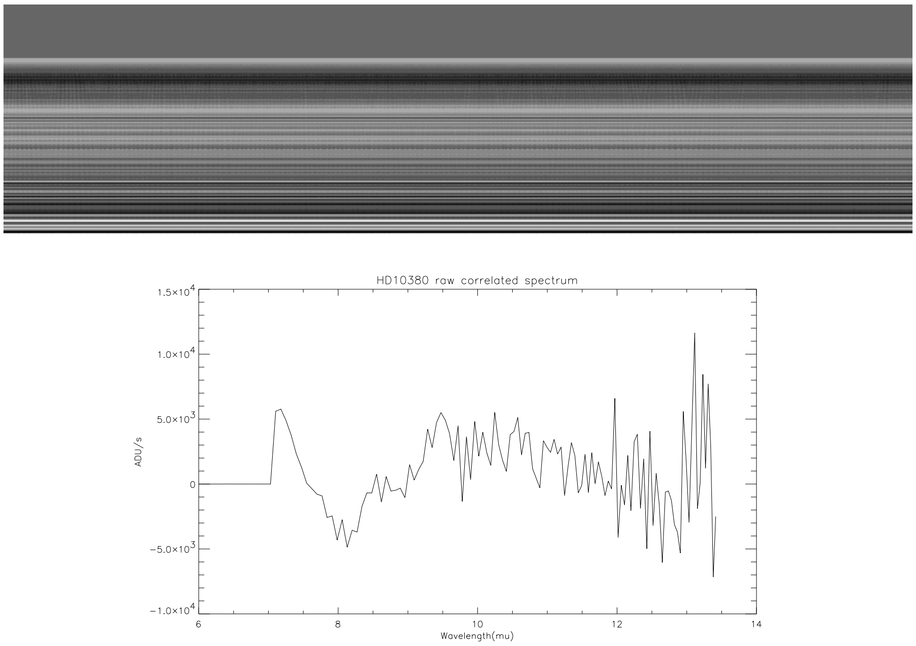

Figure 1: (a) 1000 raw compressed MIDI spectra of the calibrator HD10380 versus time (increasing toward right) and wavelength (increasing toward bottom). Wavelengths $< 7\mu$ have been suppressed. (b) A single spectrum from the series.

3.2. Background Removal

The further reduce the background we run a temporal high-pass filter over the compressed data on a pixel-by-pixel basis. In practice this is done by running a boxcar smoothing filter, of full width 50 points, over the data and subtracting this low-pass filtered data from the original data. For this to work, it is of course necessary that the signal be modulated by stepping the OPD at a rate much higher than 1 wavelength per 50 points. Typically this is $(1\lambda)/5$ points. This OPD rate can be optimized from the signal/noise point of view at any given wavelength, but for our broadband measurements we have not attempted this refinement.

In Fig. 2. we show the same data as Fig 1, but with the low temporal frequencies removed. In Fig. 2b the sinusoidal fringe is now easily visible. In Fig. 2a the broom-like pattern of fringes is caused by the imposed modulation of the OPD as it passes back and forth through the zero point.

3.3. Instrumental OPD demodulation

To remove this modulation we multiply each spectrum by $\exp(-i\ kD_i)$ as discussed in section 2. The data is now *Complex* and in Fig 3. we show the *Real* part of the result. Fig. 3a shows that the previous rapid change of slope of the fringes has been replaced by a slow drift caused by the variation in atmospheric delay. The single spectrum in Fig 3b shows at great deal of power a near zero frequency, combined with a high frequency component:the second side band frequency caused by the $\exp(ik\ (D_a + 2 * D_i))$ term.

3.4. Atmospheric Delay Estimation and Removal

Fourier transforming the spectra from Fig. 3 gets us to Figs. 4 and 5. We now have the choice between looking for the peak in the *Real* part of the signal, which is equivalent to *phase* locking in tracking terminology, or the peak in the *Absolute Value* of the signal, which is effectively *Group Delay* estimation. The first method has been discussed by J. Meisner[3] , while the second has been discussed in the literature by him and others,[4] ,[5] ,[6].[7] We

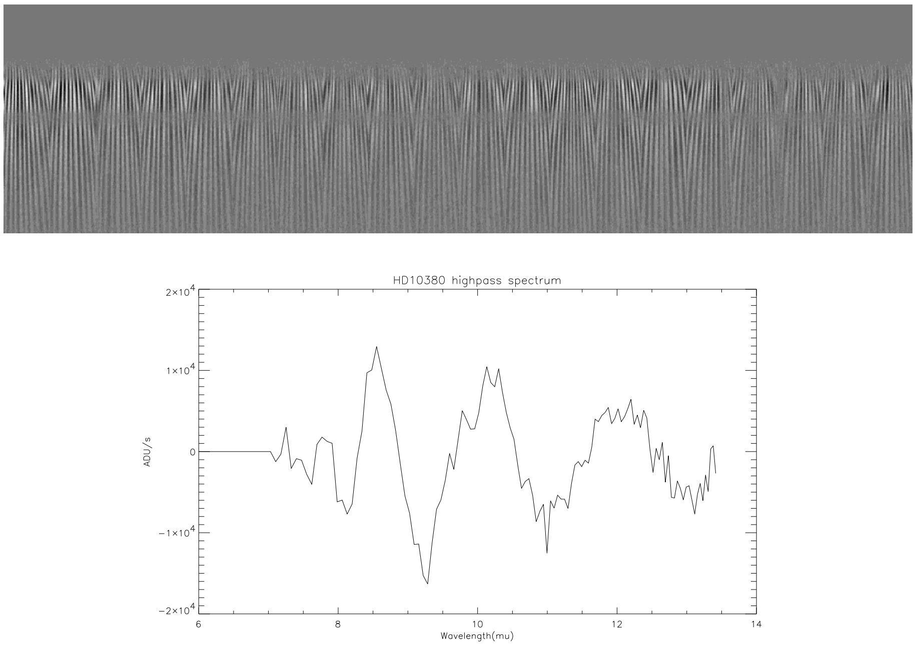

Figure 2: (a) High-pass filtered spectra. Fringes are weak at the top and just above the middle ($\lambda \sim 9.6\mu$)because of atmospheric absorption. (b) A single spectrum; the fringe is clearly visible.

have chosen the second method. Delay estimation from the phase peak gives a lower error in the high S/N case, but in cases of lower S/N has a finite probability of a large OPD error due to fringe hopping. It is also highly sensitive to changes in the atmospheric phase Φ_a due to dispersion effects that we will discuss below, while the group delay estimate is not. Figs. 4a and 5a show plots of the *Real* and *Absolute* value of the delay function as a function of delay (ordinate) and time (abscissa), while Figs 4b and 5b plot single time samples. We can easily see the **image sideband** peak drifting through the true peak, the atmospheric drift of the true peak, and variations in the overall amplitude, caused mostly by drift in the image overlap from the two telescopes. Very discerning eyes can see variations in the ratios of the sidelobes in Fig 4a due to dispersion phase variations.

In Fig. 6 we actually plot the estimated atmospheric OPD as a function of time, and see that on this day in any case, the atmosphere at Paranal was very stable. The drift over three minutes was not more than $\pm 20\mu$. Demodulating the atmospheric delay, by the same technique as applied to the instrumental delay, yields Figs. 7. Most of the "broom" pattern has disappeared, while the single spectra in Fig. 7b still show the high-frequency component due to the image frequency. This can again easily be suppressed by averaging in time, which is shown in Fig 7c.

3.5. Dispersion or "Phase" correction

We might think that removal of the group delay phase would give us "coherent" data that we could simply sum. It is sobering to look at the **phase** of the data after the delay correction, which are shown in Figs 8. The removal of the group delay has in effect made a fit to the **gradient** of phase with respect to frequency and removed this fit, leaving so-called **differential phase**. Since the source in these plots is a calibrator, under ideal conditions this differential phase should be constant and zero. There is, of course, an instrumental phase imposed on the true source phase. The instrumental phase should be almost constant in time, and relatively smooth in frequency. What we see in Fig. 8a is a fairly strong variation of phase in time on second time scales, with not much change in the frequency structure (on time scales of minutes). Almost certainly we are seeing dispersion effects, where

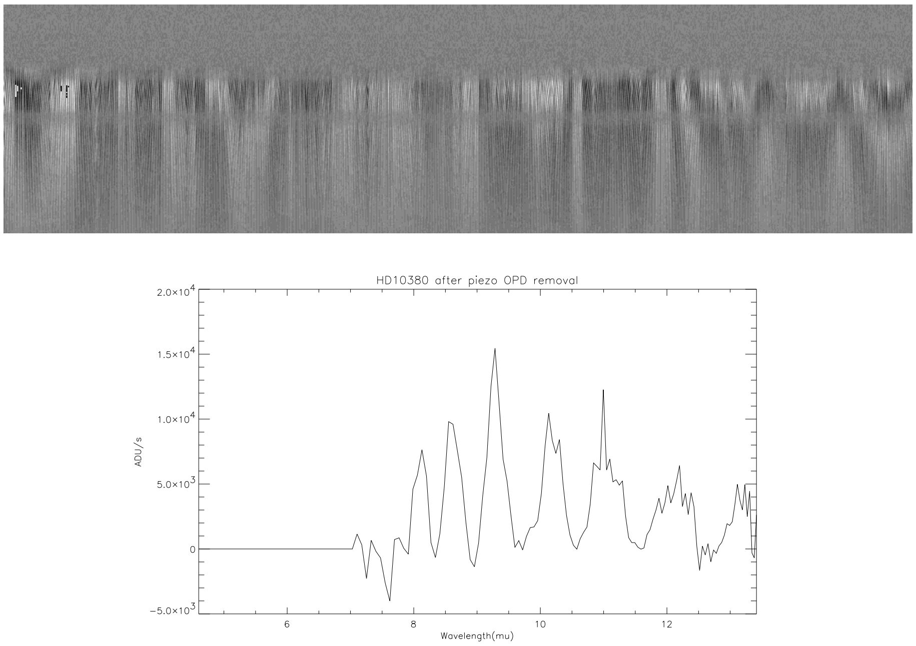

Figure 3: Data after removal of instrumental OPD. The main fringe has moved to near zero frequency and the "image" fringe is visible as a high frequency modulation.

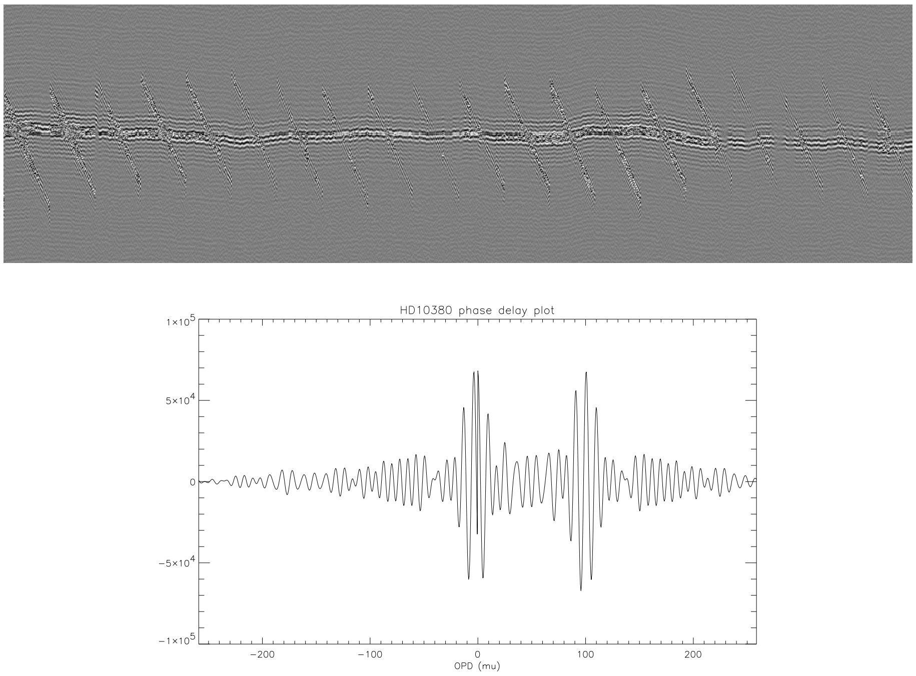

Figure 4: (a) Real part of delay function versus delay (ordinate) and time (abscissa). (b) The delay function at one time ; the true delay pattern and the image sideband pattern are both seen.

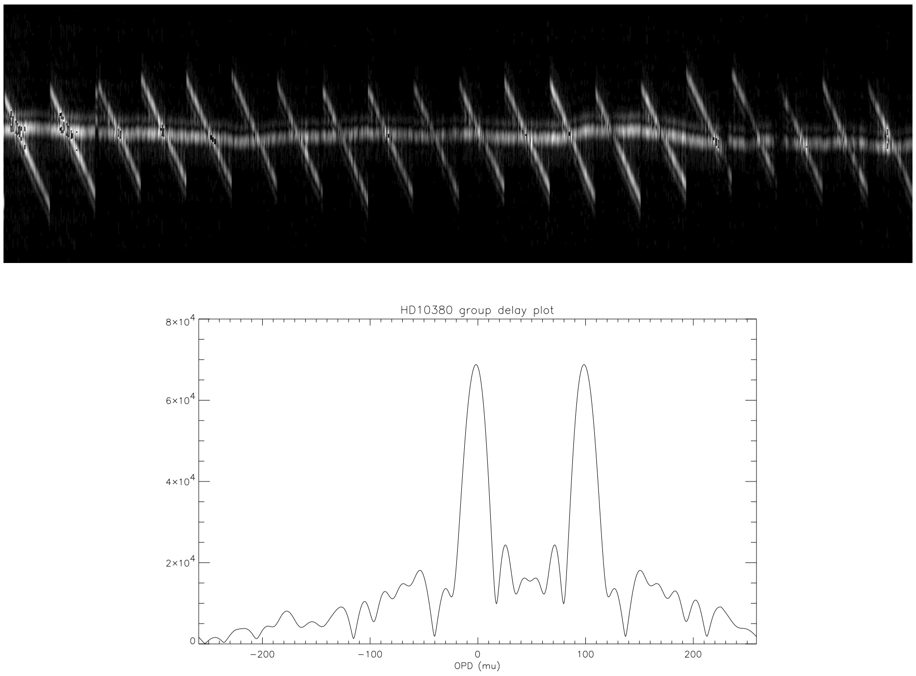

Figure 5: (a) Absolute value of delay function versus group delay. The true atmospheric D_a varies slowly, while the image sideband delay moves in a sawtooth pattern because of the modulation of D_i.

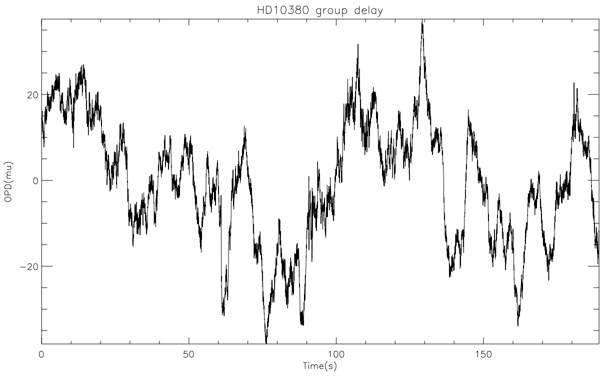

Figure 6: Estimated group delay as a function of time.

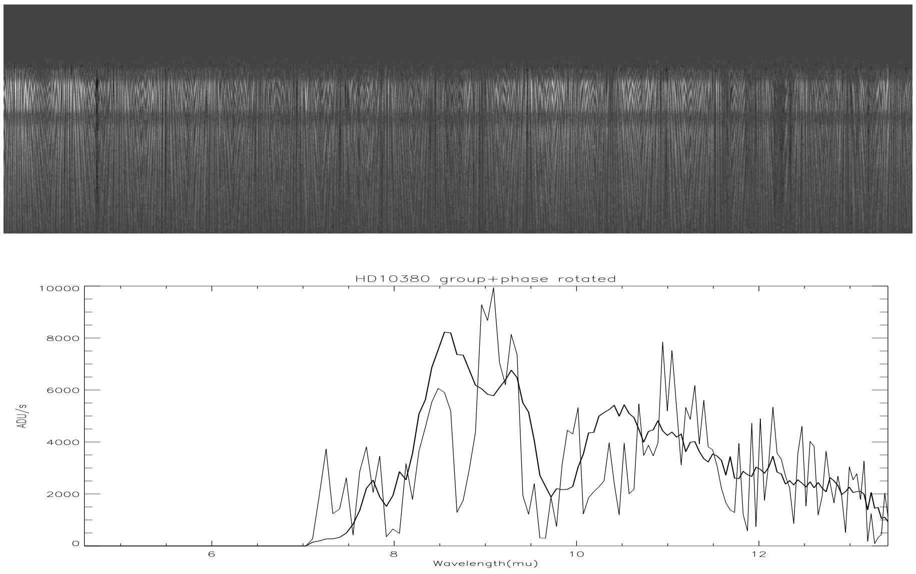

Figure 7: (a) Fringe pattern after demodulation of atmospheric delay. (b) Plots of single spectra before and after time smoothing.

the varying index of refraction of water vapor is imposing variations of phase that are not removed by the linear model of the group delay fitting. The phase shifts on times scales of a minute or two are almost constant as a function of frequency, and can be approximated as a constant phase shift over the N-band (Fig. 8b). The phase drifts are tens of degrees in a few seconds and one hundred degrees over a few minutes (Fig 9a); removing this shift is absolutely essential to coherent integration. We estimate the phase per frame as the mean phase of the complex visibilities averaged over the band, and we subtract this average phase from the complex visibility at each spectral channel. The effect of this subtraction, shown in Fig. 9b, is a smooth and stable phase structure.

The reason why a constant phase correction for dispersion works, reasonably well, is shown in Fig. 10, where I have plotted "excess phase" $(kD_a(n-1))$ as a function of frequency in the N-band for an arbitrary D and for an index of refraction n taken from models of a wet atmosphere calculated by R. Mathar. The excess phase (thick line) is close to a straight line, *whose intercept with the y-axis is not at zero phase.* Thus removal of this straight line approximation (which is what the group delay removal does), leaves a near-constant, non-zero residual, shown as a dotted line, which is what the constant-phase "dispersion" correction removes. The residual after these two steps is shown as a thin solid line, in this case multiplied by twenty for visibility. Thus the "constant phase" approximation to the dispersion removes about 98% of the total dispersion correction in phase. From the above quoted statistics, the variable part of the residuals, over a few minutes of time, are of order a few degrees in phase. The more slowly varying parts, mostly due to dispersion effects in the delay lines, should be removed by the calibration process.

For the limited number of calibrators which I have inspected, the resulting "dephased" or "dedispersed" visibilities, i.e. after removal of a phase zero and phase gradient for each frame show little variation in phase structure as a function of frequency. Thus after some flagging of suspicious points, I average these visibilities coherently over the whole observation to reach the final visibility amplitude and differential phase (Fig. 11).

4. SHORTCOMINGS AND FUTURE WORK

A few of the shortcomings in this method and their correction are obvious. For example the constant phase correction for dispersion should be replaced by a full model of the dispersion, such as those discussed by R.

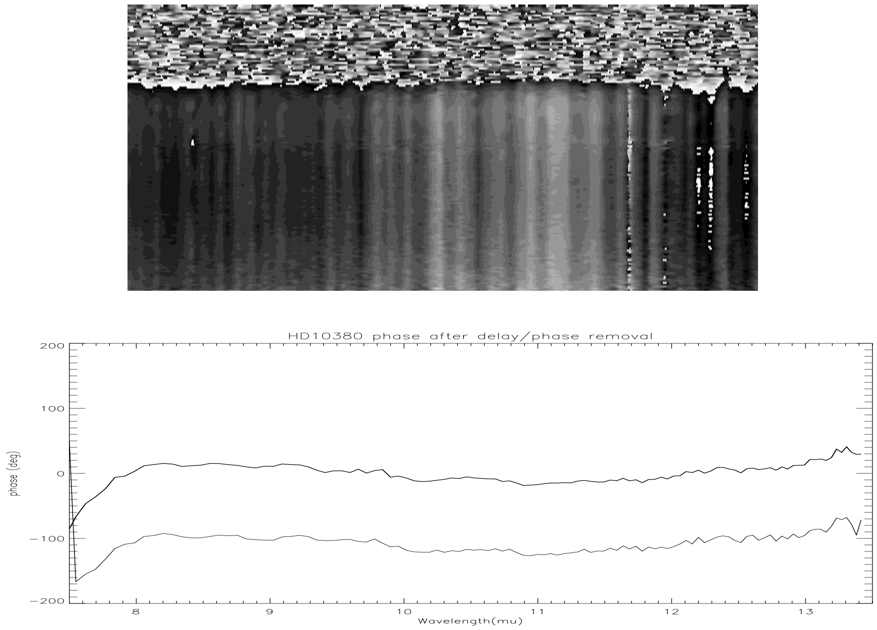

Figure 8: (a) Phase as a function of wavelength and time (b) Phase versus wavelength at two well separated times.

Tubbs and J. Meisner at this meeting. A more subtle problem is the non-calibrated loss of coherence due to delay jitter. The delay estimation error for group delay tracking will be of order $\delta D \sim \frac{\lambda^2}{\Delta\lambda S_o}$ where $\Delta\lambda$ is the bandwidth and S_o the broadband signal/noise ratio in a coherence time τ_o. The *phase tracking* error would be smaller by $\Delta\lambda/\lambda$, but this is a small improvement in the N-band, and probably not worth the tradeoff against the robustness of group delay tracking. In either case this introduces an r.m.s. phase error of order $1/S_o$ in each measurement, or a corresponding correlation loss of $\sim \exp(-1/S_o^2)$. For moderate to high values of S_o this is negligible, but it is significant for high accuracy experiments, and is not directly removed by calibration, since the signal/noise for the calibrator is usually higher than for the source.

The group delay estimation assumes *de facto* that the source was only slightly resolved, or more precisely that its visibility does not change strongly with frequency. For highly resolved sources this will not be true, and for such sources double peaks are often found in delay space. At the very least an iterative technique has to be used for these sources: after a first estimate of the group delay and correlated flux have been made, the the group delay shoud not be estimated from the position of the peak, but from a fit of the delay function to a PSF created from the Fourier Transform of the correlated flux.

The coherent method as a whole will not work for $S_o <\sim 5$ for in this case the group delay cannot be reliably determined. One can push this limit slightly lower by modelling the behavior of D_a with *a priori* assumption on its statistics.[3] A more direct and easy to implement scheme is to Fourier transform the spectral fringes in **two** dimensions, frequency and time. The peak of the resulting function represents the best simultaneous fit to both D_a and dD_a/dt.

ACKNOWLEDGMENTS

I wish to thank J. Meisner for many discussion leading to the implementation of the method shown here.

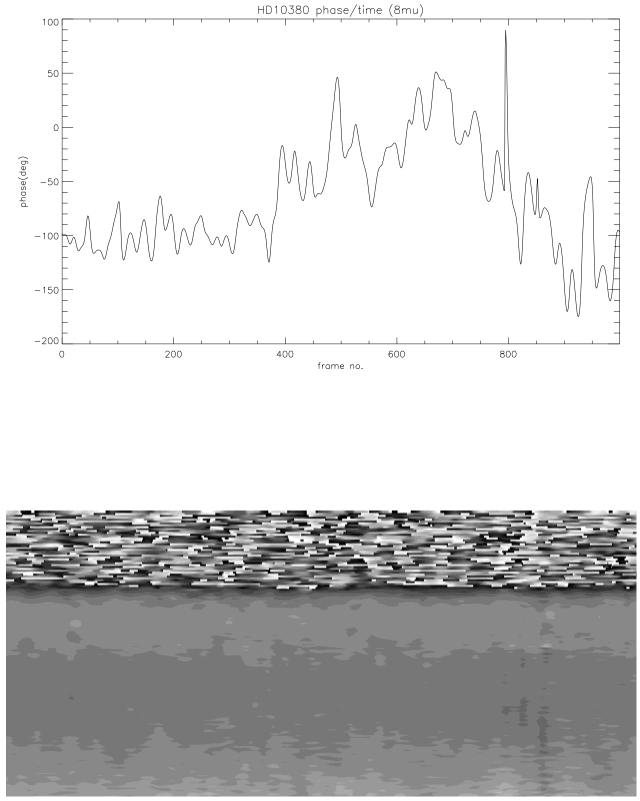

Figure 9: (a) Phase or dispersion correction as a function of time. (b) Phase versus time and wavelength after removal of constant-phase dispersion correction

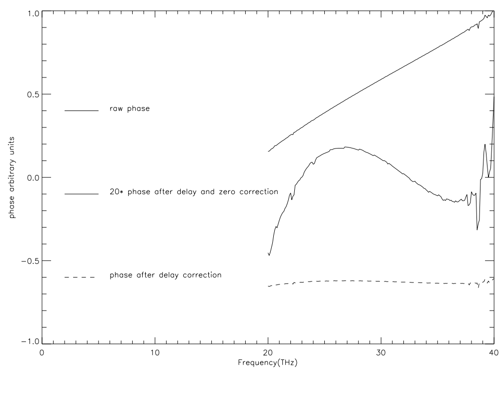

Figure 10: Excess phase versus frequency from models by R. Mathar

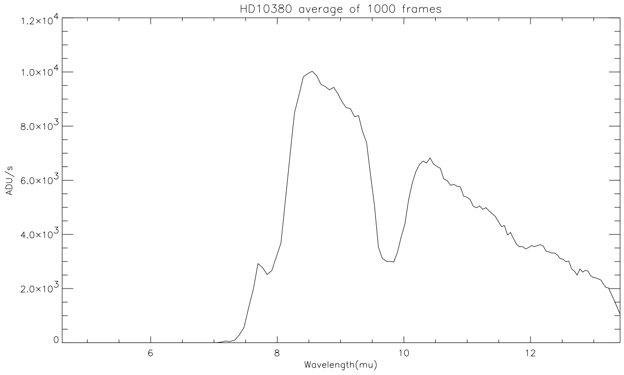

Figure 11: Correlated flux versus wavelength averaged over the entire observation. The structure in the spectrum is due to the Rayleigh-Jeans spectrum of the hot stellar source and atmospheric absorption, including the O_3 lines at 9.6μ.

REFERENCES

1. C. Leinert *et al.*, "Ten-micron instrument MIDI: getting ready for observations on the VLTI," *Proc. SPIE* **4838**, pp. 893–904, 2003.
2. Glindemann, A. *et al.*, "The VLTI– A Status Report," *Proc. SPIE* **4838**, pp. 89–100, 2003.
3. J. Meisner, *Estimation and Tracking of Atmospheric Delay Noise in a Long-Baseline Optical Stellar Interferometer and Determination of the Expected Estimation Error*. PhD thesis, University of Minnesota, 1995.
4. J. Meisner, "Fringe tracking and group delay tracking methods for MIDI," *Liège International Astrophysics Colloquium*(36), pp. 225–231, 2001.
5. C. Lawson, P. R. Scott T. R. Hannif, "Group-delay tracking and visibility fluctuations in long-baseline stellar interferometry," *Monthly Notices of the Royal Astronomical Society* **304**, pp. 218–224, 1999.
6. T. A. ten Brummelaar, "Correlation measurement and group delay tracking in optical stellar interferometry with a noisy detector," *Monthly Notices of the Royal Astronomical Society* **285**, pp. 135–150, 1997.
7. P. R. Lawson, "Group delay tracking in optical stellar interferometry with the fast Fourier transform," *J. Opt. Soc. Am. A* **12**, pp. 366–374, 1995.